Reprinted from
Journal of Imaging Science and Technology® 62(4): 040409-1–040409-5, 2018.

Inkjet Printing and Intense Pulsed Light Sintering of Multiwall Carbon Nanotubes for Sensor Applications

Dana Mitra and Tatiana Zubkova
Technische Universität Chemnitz, Digital Printing and Imaging Technology, Chemnitz, Germany
E-mail: dana.mitra@mb.tu-chemnitz.de

Carina Gerlach and Olfa Kanoun
Technische Universität Chemnitz, Professorship of Electrical Measurements and Sensor Technology, Chemnitz, Germany

Dominique Miesel and Heinrich Lang
Technische Universität Chemnitz, Professorship of Inorganic Chemistry, Chemnitz, Germany

Reinhard R. Baumann▲
Technische Universität Chemnitz, Digital Printing and Imaging Technology, Chemnitz, Germany
Fraunhofer Institute for Electronic Nano Systems (ENAS), Department Printed Functionalities, Chemnitz, Germany

Abstract. *Fully inkjet-printed multiwall carbon nanotube (MWCNT) layers and their feasibility towards the implementation as a low cost and flexible sensing element is reported. The focus is set on the resistive behavior of the carbon nanotubes (CNTs) and the adjustability towards a defined target range. To realize the sensors on a low cost and high flexible polyethylene terephthalate (PET) foil, the intense pulsed light (IPL) sintering is introduced to achieve the required performance for both the CNT dispersion as well as the silver electrodes. The very novel topic of the simultaneous photonic sintering of a two-material layer stack and the involved challenges are demonstrated. The MWCNT dispersion was successfully printed with the inkjet printing technology and functionalized by thermal and IPL sintering methods, achieving a resistance of* 100 kΩ *in the target area (*1 kΩ *to* 1 MΩ*) for the sensor. The dependence of the resistance on parameters like number of CNT overprints, the pattern layout as well as the post-treatment methodology is analyzed in detail. These results can be further employed for the development of CNT-based sensor elements and the change in their resistance caused by environmental conditions. In addition, such single sensors raise the opportunity of a combination to a sensor matrix to demonstrate the integration in applications such as a shoe sole (proof of concept) but primarily for medical applications e.g., in mattresses in hospitals for constant recording of bedfast or comatose patients.* © *2018 Society for Imaging Science and Technology.*
[DOI: 10.2352/J.ImagingSci.Technol.2018.62.4.040409]

1. INTRODUCTION

Thin and flexible printed electronics are of great interest due to their various advantages such as high flexibility, low cost fabrication and adaptability towards various integrations. [1–3] In the field of healthcare, especially wearable electronic components, tracking the real-time health status are of major importance either directly manufactured on wearable substrates/surfaces or on thin, flexible substrates suitable for the integration in wearable applications. Such printed sensing elements can be based on materials like graphene or carbon nanotubes (CNTs) [4–8].

Especially the inkjet printing technology features high potential due to its minimized material consumption, high accuracy, non-contact printing as well as processing under ambient conditions.

To allow the utilization of high flexible, but mostly temperature-instable polymeric foils or even textiles, next to the traditional thermal sintering method the novel intense pulsed light (IPL) sintering process demonstrates high potential in the functionalization of metallic and also various other materials [9–16].

Therefore, the feasibility of the inkjet printing technology for the development of a flexible and thin sensor element, based on multiwall carbon nanotubes (MWCNTs), has been investigated in this research. Furthermore, to allow the manufacturing on temperature-instable polymeric foils like polyethylene terephthalate (PET), IPL sintering was introduced for the post-treatment of both, the silver electrodes and the CNT layers and compared to the results of the thermal sintering.

Various pattern designs were implemented by adjusting the electrode size and distance as well as the correlated CNT pattern. Additionally, the printing and sintering parameters, such as number of layers, drying and sintering methodology, of the CNT layer were varied, to investigate the change in resistance and their impact on the sensing properties. Additionally, an analysis of defects, their origin as well as overcoming them are discussed.

▲ IS&T Member.

Received Mar. 1, 2018; accepted for publication June 21, 2018; published online Aug. 6, 2018. Associate Editor: Kye-Si Kwon.
1062-3701/2018/62(4)/040409/5/$25.00

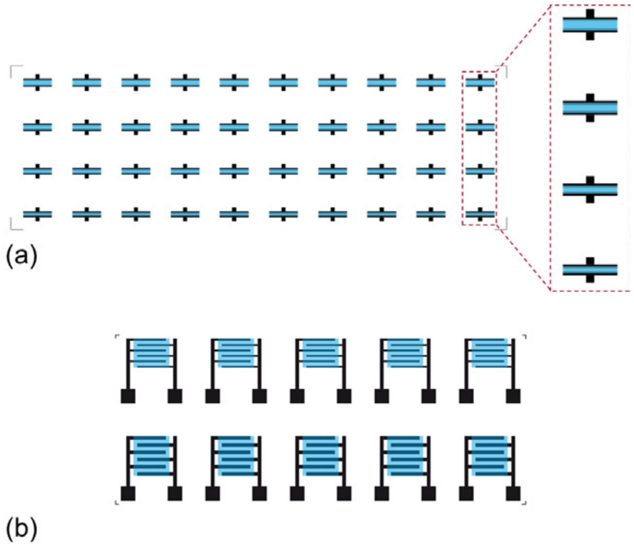

Figure 1. Digital patterns: (a) two-finger electrode for basic investigations; (b) six-finger electrode for sensor application.

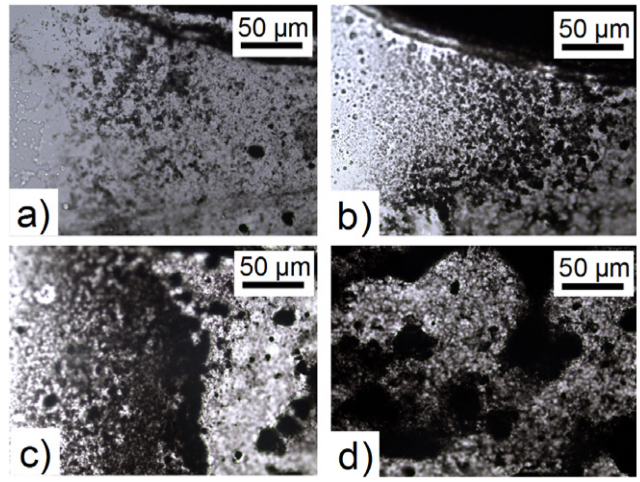

Figure 2. Microscopic images of the CNT distribution as a function of CNT overprints, thermally sintered at 150°C for 60 min: (a) 10 layers; (b) 20 layers; (c) 30 layers; (d) 40 layers.

2. MATERIALS AND METHODS

Two digital patterns were implemented, which are a simple two-finger electrode pattern (Figure 1a) for a basic investigation of the electrical performance of the CNTs and a more complex six-finger interdigitated electrode (Fig. 1b).

The MWCNTs were bought from Sigma Aldrich with a diameter of 20–40 nm and a length of 1–2 µm. To achieve a stable dispersion and suitable for the inkjet printing process, the CNTs were functionalized with COOH groups by sonication in concentrated HNO_3 and H_2SO_4. The CNTs were finally dispersed with 0.05 wt.% in isopropanol. The dispersion was stable for several days without sedimentation of the CNTs. Slight sedimentation was recovered by a sonication even after several weeks. For the silver electrodes a nanoparticle silver ink was used: DGP-40LT-15C from Advanced Nano Products ANP. The substrate was the PET foil Melinex 401 from DuPont Teijin Films with a thickness of 100 µm. Printing was carried out with the Dimatix Materials Printer DMP2831 from FUJIFILM Dimatix. For sintering two methods were used, which are the thermal sintering in an oven and the IPL sintering (PulseForge 3200 from Novacentrix).

The research includes microscopic images (light microscope DM4000, from Leica), surface profiles by surface topographic scans with mechanical contact (profilometer Dektak 150 by Veeco,) and electrical measurements (resistance by a two-point method with a manual probe system PM5, Süss Microtec).

3. RESULTS AND DISCUSSION

First, the CNTs were characterized with a light microscope toward their layer formation and homogeneity. Thus, several layers up to 40 were printed on top of each other, to evaluate the CNT layer formation with the goal of an even CNT distribution to ensure a reliable and generally present resistance within a defined range of $1\ \mathrm{k\Omega} < x < 1\ \mathrm{M\Omega}$. Additionally, two sintering methodologies were implemented and the resistance of the CNT layers was measured between the silver electrodes.

Based on this, the final CNT printing parameters (pattern design, number of layers, and post-treatment) were defined for the implementation in a sensor layout.

3.1 *Optical Investigation of the MWCNT Layers*

The CNT–isopropanol dispersion was successfully inkjet-printed with 0.05 wt.% and various number of CNT overprints. Their distribution is optically analyzed in Figure 2.

The overall distribution of the CNTs appears very inhomogeneous with material accumulations and uncovered areas in between. This irregularity increases with increasing number of CNT overprints and therefore with increasing material amount. Also, the drop ejection was not yet optimized. Challenges like satellite drops, angular drop offset, and non-working nozzles might impact the overall performance and need to be adjusted. Therefore, the number of overprints was decided to not exceed 30 layers, which appeared to be enough material to achieve a resistance in the target range of $1\ \mathrm{k\Omega} < x < 1\ \mathrm{M\Omega}$ and to reduce the time efforts by printing many layers on top of each other.

To improve the homogeneity of the CNT layer, the drop ejection was adapted and the printing table (and therefore the substrate) was heated to 45°C, which will lead to faster solvent evaporation and might avoid the washing away of the previously deposited CNT material. The results of the full electrode–CNT stack with 20 and 30 layers of CNT overprints are presented in Figure 3 with a magnification on the CNT distribution in Figure 4.

The silver layer was post-treated with the IPL sintering at 0.82 J cm^2 for 1 ms and the CNT–isopropanol dispersion was printed afterwards in between the electrodes with a slight overlap to the silver electrodes, to ensure an appropriate contacting. The layer homogeneity of the CNT distribution

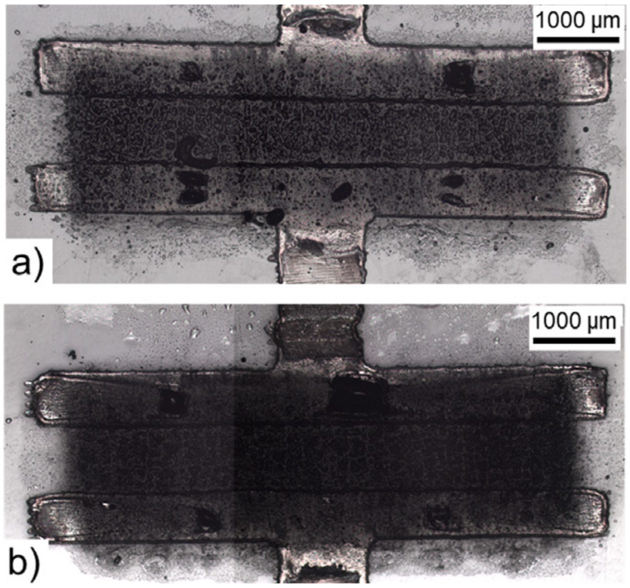

Figure 3. Microscopic images of the printed silver electrodes (IPL sintered at 0.82 J/cm^2 for 1 ms) with a digital distance of 1.5 mm and printed CNT layers in between with an overlapping area on the silver electrodes (IPL sintered at 0.82 J/cm^2 for 1 ms): (a) 20 CNT layers; (b) 30 CNT layers.

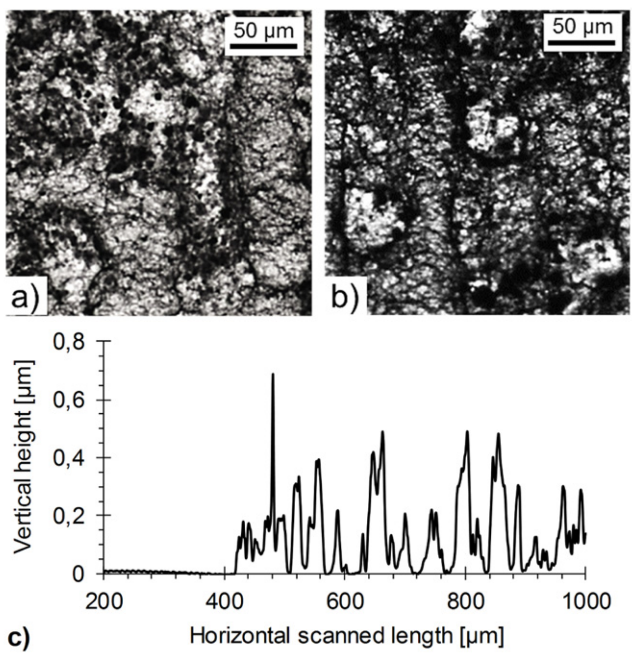

Figure 4. Microscopic images of the CNT distribution as a function of CNT overprints after optimization with respect to the drop ejection and the application of table heat 45°C, thermally sintered at 150°C for 60 min: (a) 20 layers; (b) 30 layers; (c) surface profile of 20 CNT layers on glass.

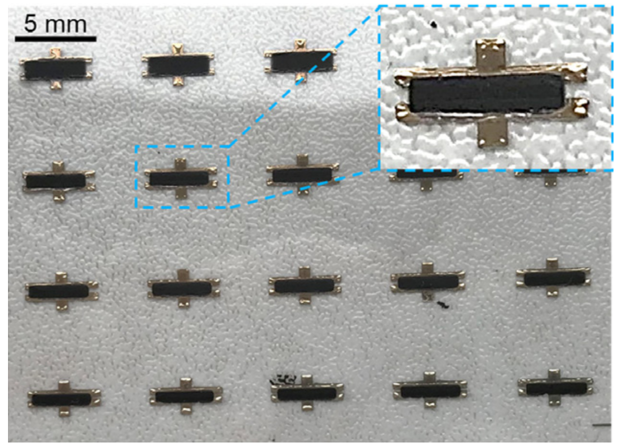

Figure 5. Array of fully inkjet-printed CNT–silver electrodes after IPL sintering at 0.71 J cm^2 for 1 ms.

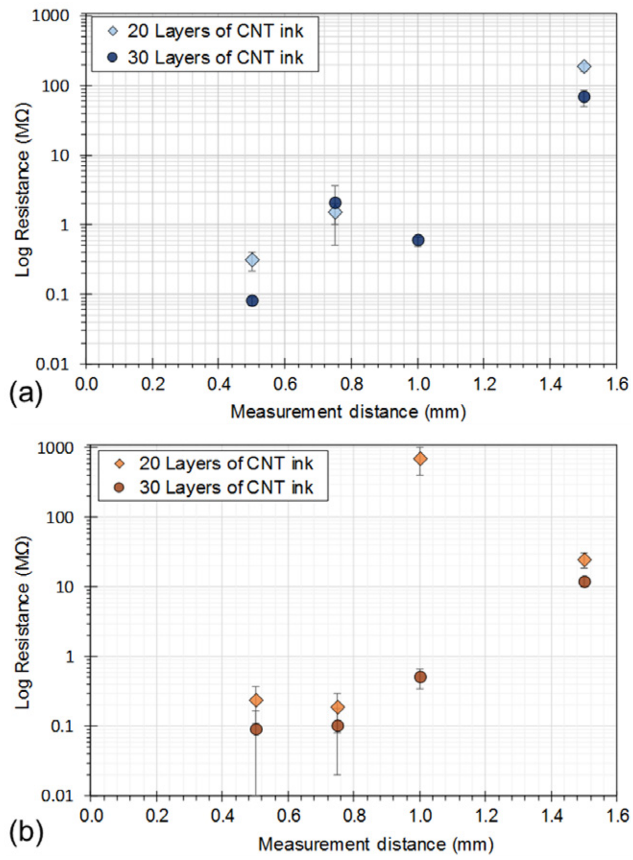

Figure 6. Average resistance of the CNT layer in dependence on the electrode design (measurement distance), number of CNT overprints and post-treatment methodology: (a) thermal sintering at 150°C for 60 min; (b) IPL sintering at 0.82 J/cm^2 for 1 ms.

seems to be more uniform, especially when comparing 30 layers of CNT from Fig. 2(c) and Fig. 4(b). Nonetheless, the overall impression of the CNT layer discloses a huge amount of satellite drops, which spread over the whole electrode pattern and might cause fluctuations within the CNT resistance and therefore in the later working/measuring of the printed sensor. For further optimization, these satellite drops will be reduced and even fully avoided, by the waveform adjustment.

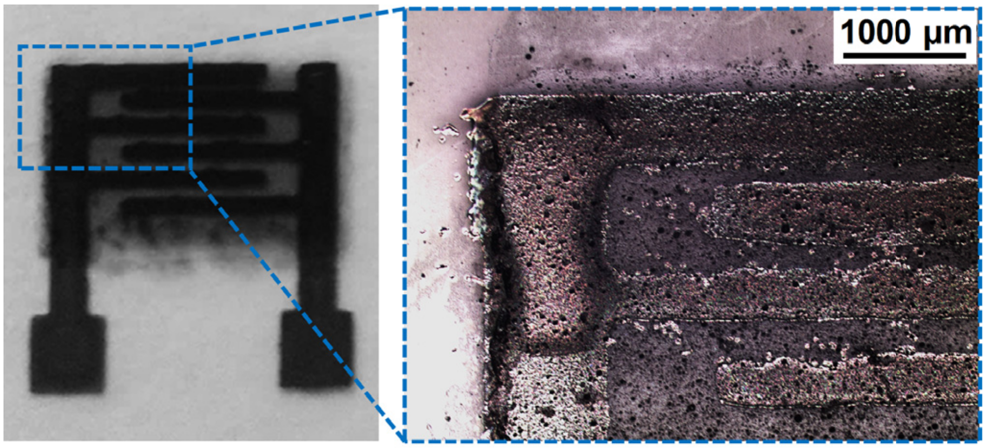

Figure 7. 10 CNT layers inkjet-printed on top of previously printed and sintered silver electrodes, both thermally sintered at 150°C for 20 minutes.

Furthermore, the IPL sintering caused slight defects in the silver layer (small blisters), but no damage to the CNT layer. The defects within the silver layer are due to minor inhomogeneous material accumulations, which might not have a direct impact on the functionality in this application here, but such unevenness in the layer thickness presents a working point in the IPL sintering, which demands layers as smooth as possible for a reliable sintering result.

In the example of the surface profile (Fig. 4c) of 20 CNT layers the high fluctuation in the distribution and layer thickness is visible, which makes it not possible to calculate a reliable average conductivity.

In addition, flashing two different materials simultaneously, in this case the silver nanoparticles and the CNTs represents a great challenge. The previous IPL sintered silver layer experiences the IPL treatment twice. Therefore, the IPL parameter of the second flash has to be adjusted to both materials, so that the first already sintered layer is not burned and the second layer is sufficiently sintered for the required structural and functional properties.

An example of a CNT–silver electrode array after IPL sintering is presented in Figure 5. The CNT printing was optimized regarding the printing parameters, that is elimination of satellite drops and clogged nozzles, as well as improved layer formation by a slow drying process.

Here it can be seen that the CNT layer (10 layers on top of each other) reveals no defects, while the silver layer identifies small blisters, which needs to be considered toward the impact on the later device functionality and reliability.

3.1.1 *Electrical Investigation of the MWCNT Layers*

The line resistance of the CNT layers between the two silver electrodes was measured (Figure 6). The resistance is displayed as a function of the electrode distance, number of CNT layers, and post-treatment method. Due to the existence of a thin layer for 10 CNT overprints and high inhomogeneity for 40 layers and more (see Fig. 2), the resistance could not be reliably measured for 10 and 40 layers. Therefore, in the graph only 20 and 30 layers of CNTs are presented and discussed.

From both graphs it can be clearly seen, that as expected, the resistance increases with increasing electrode distance. Also, printing 30 layers of CNTs on top of each other, results in a further less resistance. The standard deviation is for most of the samples for the thermal sintering (Fig. 6a) within a range of 10%–30%. The importance and acceptable fluctuation of these deviations are defined by the sensitivity and effective range of the respective sensor.

The high standard deviation for the IPL sintered samples might be either caused by the CNT layer distribution or by defects at the edge of the silver layer induced by the IPL treatment and discussed in the chapter "*Optical investigation as a function of the number of MWCNT layers*." However, despite the high deviation, the overall resistance was in a similar range or lower than the thermally sintered CNT stacks.

3.2 *Toward Sensor Applications*

For a proof of concept, the CNT–silver layer stack, as presented in the digital image from Fig. 1(b), was printed and thermally sintered at 150°C for 20 min (Figure 7) and analyzed for a temperature response by a resistance change. It was found that the resistance drops between 5% and 12% on increasing the temperature from 10°C up to 80°C, and increases back to the initial value when lowering the temperature back to 10°C. The total measurement time for this first proof record was comparable slow (one complete cycle was of 15 h). Further investigations will be carried out to identify the response time of the printed sensor.

4. CONCLUSIONS

It was shown that a self-made MWCNT–isopropanol dispersion could be successfully inkjet-printed and functionalized on a flexible and thermally instable PET foil.

The printed CNT layers revealed partly inhomogeneous distributions, which depends strongly on the deposited material amount as well as printing parameters, like table temperature and stable drop ejection. The homogeneity of the CNT layers was optimized accordingly followed by a functionalization by means of thermal and IPL sintering methods. Both sintering methodologies resulted in a resistive CNT layer within the range of several $M\Omega$ down to 100 kΩ in dependence on the implemented layout and CNT material amount (overprints).

Furthermore, it was shown that the IPL sintering is feasible to be applied on a two-material layer stack, but needs to be adapted according to the limits of both materials.

ACKNOWLEDGMENT

This research work was financially supported by the ESF (Europa Fördert Sachsen - Europäischer Sozialfonds) and the Europäische Union funded project "SenseCare" (FKZ 100270070). The authors would like to thank Mr. Aakash Grewal from Technische Universität Chemnitz for his support in the Inkjet Printing and characterization.

REFERENCES

[1] A. Teichler, "Inkjet printing of organic electronics – comparison of deposition techniques and state-of-the-art developments," J. Mater. Chem. C **1**, 1910–1925 (2013).

[2] J. Perelaer, P. J. Smith, D. Mager, D. Soltman, S. K. Volkman, V. Subramanian, J. G. Korvink, and U. S. Schubert, "Printed electronics: the challenges involved in printing devices, interconnects, and contacts based on inorganic materials," J. Mater. Chem. **20**, 8446–8453 (2010).

[3] K. Li, J. K. Liu, W. S. Chen, and L. Zhang, "Controllable printing droplets on demand by piezoelectric inkjet: applications and methods," Microsyst. Technol. **24**, 879–889 (2018).

[4] N. T. Dinh, E. Sowade, T. Blaudeck, S. Hermann, R. D. Rodriguez, D. R. Zahn, S. E. Schulz, R. R. Baumann, and O. Kanoun, "High-resolution inkjet printing of conductive carbon nanotube twin lines utilizing evaporation-driven self-assembly," Carbon **96**, 382–393 (2016).

[5] P. Lorwongtragool, E. Sowade, N. Watthanawisuth, R. R. Baumann, and T. Kerdcharoen, "A novel wearable electronic nose for healthcare based on flexible printed chemical sensor array," Sensors **14**, 19700–19712 (2014).

[6] O.-S. Kwon, H. Kim, H. Ko, J. Lee, B. Lee, C.-H. Jung, J.-H. Choi, and K. Shin, "Fabrication and characterization of inkjet-printed carbon nanotube electrode patterns on paper," Carbon **58**, 116–127 (2013).

[7] A. Denneulin, J. Bras, F. Carcone, C. Neuman, and A. Blayo, "Impact of ink formulation on carbon nanotube network organization within inkjet-printed conductive films," Carbon **49**, 2603–2614 (2011).

[8] S. K. Eshkalak, A. Chinnappan, W. A. D. M. Jayathilaka, M. Khatibzadeh, E. Kowsari, and S. Ramakrishna, "A review on inkjet printing of CNT composites for smart applications," Appl. Mater. Today **9**, 372–386 (2017).

[9] J. R. Greer and R. A. Street, "Thermal cure effects on electrical performance of nanoparticle silver inks," Acta Mater. **55**, 6345–6349 (2007).

[10] G. Vandevenne, W. Marchal, I. Verboven, J. Drijkoningen, J. D'Haen, M. K. Van Bael, A. Hardy, and W. Deferme, "A study on the thermal sintering process of silver nanoparticle inkjet inks to achieve smooth and highly conducting silver layers," Phys. Status Solidi A **213**, 1403–1409 (2016).

[11] D. Mitra, K. Y. Mitra, M. Hartwig, and R. R. Baumann, "Intense pulsed light sintering of an inkjet printed silver nanoparticle ink depending on the spectral absorption and reflection of the background," J. Imaging Sci. Technol. **60** (2016).

[12] P. Gokhale, D. Mitra, E. Sowade, K. Y. Mitra, H. Gomes, E. Ramon, A. Al-Hamry, O. Kanoun, and R. R. Baumann, " Controlling the crack formation in inkjet-printed silver nanoparticle thin-films for high resolution patterning using intense pulsed light treatment," Nanotechnology **28**, 495301 (2017).

[13] S. Wünscher, R. Abbel, J. Perelaer, and U. S. Schubert, "Progress of alternative sintering approaches of inkjet-printed metal inks and their application for manufacturing of flexible electronic devices," J. Mater. Chem. C **28**, 10232–10261 (2014).

[14] L. Rebohle, S. Prucnal, and W. Skorupa, "A review of thermal processing in the subsecond rang: semiconductors and beyond," Semicond. Sci. Technol. **31**, 103001 (2016).

[15] H. Kang, E. Sowade, and R. R. Baumann, "Direct intense pulsed light sintering of inkjet-printed copper oxide layers within six milliseconds," ACS Appl. Mater. Interfaces **6**, 1682–1687 (2014).

[16] N. Marjanovic, J. Hammerschmidt, J. Perelaer, S. Farnsworth, I. Rawson, M. Kus, E. Yenel, S. Tilki, U. S. Schubert, and R. R. Baumann, "Inkjet printing and low temperature sintering of CuO and CdS as functional electronic layers and Schottky diodes," J. Mater. Chem. **21**, 13634–13639 (2011).